AIP | Review of Scientific Instruments

Fluorescence temperature sensing on rotating samples in the cryogenic range

F. Bresson and R. Devillers

Citation: Review of Scientific Instruments **70**, 3046 (1999); doi: 10.1063/1.1149866
View online: http://dx.doi.org/10.1063/1.1149866
View Table of Contents: http://scitation.aip.org/content/aip/journal/rsi/70/7?ver=pdfcov
Published by the AIP Publishing

Fluorescence temperature sensing on rotating samples in the cryogenic range

F. Bresson[a] and R. Devillers
Laboratoire d'Optique P. M. Duffieux, UMR 6603, Université de Franche–Comté, 25030 Besançon, France

(Received 20 January 1999; accepted for publication 12 April 1999)

A surface temperature measurement technique for rotating samples is proposed. It is based on the concept of fluorescence thermometry. The fluorescent and phosphorescent phenomena have been applied in thermometry for ambient and high-temperature measurement but not the cryogenic domain, which is explored using thermocouple- or platinum resistor-based thermometers. However, thermal behavior of Yb^{2+} ions in fluoride matrices seems to be interesting for thermometry in the range 20–120 K. We present here a remote sensing method which uses fluorescence behavior of Yb^{2+} ion-doped fluoride crystals. The fluorescence decay time of such crystals is related to its temperature. Since we developed a specific sol–gel process (OrMoSils) to make strongly adherent fluorescent layers, we applied the fluorescence thermometry method for rotating object surface temperature measurement. The main application is the monitoring of surface temperature of the ball bearing or turbopump axis in liquid propulsion rocket engines. Our method is presented and discussed, and we give some experimental results. An accurate calibration of the decay time of $CaF_2:Yb^{2+}$ versus temperature is also given. © *1999 American Institute of Physics.* [S0034-6748(99)04107-6]

I. INTRODUCTION

Fluorescence phenomenon has already been demonstrated to be a suitable means for temperature measurement. Grattan and co-workers developed many thermometers based on the fluorescence of Cr^{3+} ions in LiSAF, garnet, or alexandrite matrices.[1–3] The temperature dependence of the fluorescence decay time of such dyes is an accurate way of measuring the temperature between about 200 and 800 K. Rare-earth-like Nd^{3+} is another interesting candidate for fluorescence thermometry in the high-temperature domain.[4] Nevertheless, the cryogenic range is generally explored using thermoelectric effect thermometers (thermocouples or platinum resistors). Recent studies regarding the fluorescence of Yb^{2+} ions in fluoride matrices show that $CaF_2:Yb^{2+}$ or $SrF_2:Yb^{2+}$ is an efficient amplifier media for solid-state laser applications. An interesting temperature dependence of the efficiency and decay time of fluorescence has been pointed out for the cryogenic range.[5] This lead us to incorporate $CaF_2:Yb^{2+}$ and $SrF_2:Yb^{2+}$ dyes in fluorescent temperature probes for cryogenic fluids. The thermal decay time dependence was used rather than thermal efficiency dependence, as it was not sensitive to the intensity fluctuations of the excitation signal. $SrF_2:Yb^{2+}$ and $CaF_2:Yb^{2+}$ present good sensitivity and efficiency, respectively, between 20 and 60 K, and between 60 and 120 K. The combination of both dyes results in an accurate fluid temperature measure in the liquid-oxygen and -hydrogen domain (20–120 K). The goal is to monitor the temperature while the liquid hydrogen (or oxygen) is getting in the admission valve that controls the liquid propulsion rocket engines.[6,7] Compared to the widely used thermocouple techniques, the optical intrinsic electromagnetic immunity was balanced by high cost and weight. Actually, the method is restricted to some measurement points which require high precision, and carried out in land trials. However, the optical-based measurement method allows remote sensing. Another interest of thermometry in the cryogenic range is the monitoring of the rocket engine turbopump axis and ball bearing temperature. We present here a remote sensing technique for measurement of the rotating sample surface temperature. Thermocouples are not suitable for this specific application since it make uses of electrical contacts. Our method is seen as the only alternative to computer simulations in this particular case.

II. PRINCIPLE

The method is based on the thermal dependence of the fluorescent decay time of $CaF_2:Yb^{2+}$ and $SrF_2:Yb^2$ dyes. The fluorescent dye is deposited on the rotating sample surface, and an optical probe is put near the layer. The probe consists mainly of a set of optical fibers, one excitation channel, and almost two detection channels. It is positioned in such a manner that the layer intersects the optical axis of each fiber during its rotation, as shown in Fig. 1. When the layer is in front of the optical axis of the excitation channel, an UV excitation pulse is triggered and propagates towards the layer. Sequentially, each detection channel collects a pulse signal as the induced fluorescence source moves along the distance d (distance between each channel), and is in front of its optical axis. If we assume that the fiber core radius is small compared to d, the signal is close to the sampled exponential decreasing fluorescence signal, with a sample frequency f, as shown in Fig. 2. The sampling fre-

[a]Electronic mail: mjacquot@utinam.univ-fcomte.fr

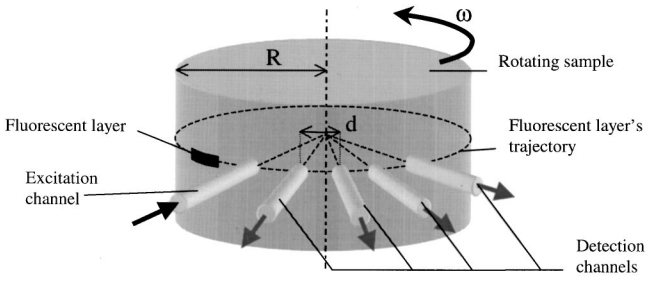

FIG. 1. Principle of the fluorescence thermometry in rotating samples. A fluorescent layer is deposited on the sample. An UV pulse is trigged while the layer is in front of the excitation channel, and the fluorescent pulses are collected as the layer moves in front of the detection channels.

quency f depends on the sample radius R, the rotating speed ω of the sample, and d (cf. Fig. 1), according to relation (1):

$$\mathbf{f}=\omega\mathbf{R}/\mathbf{d}. \tag{1}$$

The envelop of the collected fluorescent signal is the fluorescence exponential decreasing law of the layer. Two points are sufficient to get the fluorescence decay time τ. If there are more than two points, τ can be calculated with an interpolation method.

The fluorescent layer has to fulfill several requirements such as supporting mechanical and chemical strains (thermal shocks, liquid flows, liquid oxygen). The geometry of the probe has to take into account some incompatible basic aspects. First, the number of detection channels (and so, the number of points) must be great, while the probe must be small enough to be incorporated in the measurement bench. Second, the distance between each channel must be as small as possible (to get points in the beginning of the fluorescent curve), but it cannot be smaller than the fiber's external diameter.

The experimental bench is a cryotribometer that simulates ball bearing friction in the cryogenic range. It is mainly constituted by two independent pins and a nitrogen tank. Each pin is fitted by a disk, as shown in Fig. 3. The left disk (test disk) is a cylinder. The right disk (strain disk) is a tore. The test disk is fitted by a set of thermocouples laid along the radius. This device allows us to calculate the surface temperature, neglecting the influence of the layer (surface temperature gradients). The precision of this method is about 0.5 K, since there are no surface temperature gradients. It falls in the other case. The left pin is fitted by an electrical resistance, giving a warm source. Each pin can rotate independently to put the strain disk in friction with the test disk in the liquid-nitrogen tank that can increase the surface temperature of the test disk. The electrical resistance can also increase the sample temperature from 77 to about 150 K without friction. The rotating speed can be adjusted from 0 to about 5000 rpm, and an induction tachymeter system gives the rotating speed with an error of less than 1 rpm.

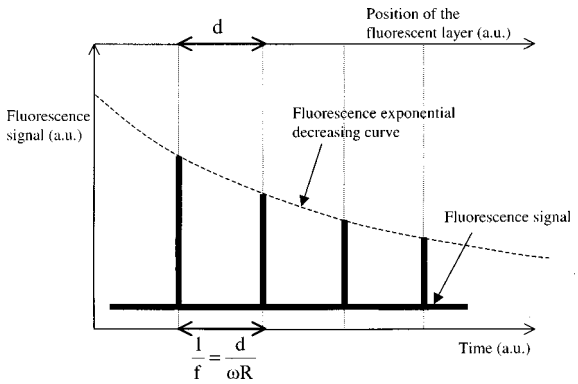

FIG. 2. Shape of the fluorescent signal obtained with a five-channel probe (full line). The dotted line is the exponential decreasing law of the fluorescence emiting source. It constitutes the envelop of the fluorescent signal. If the pulses are sharp enough, the signal is close to the sampled exponential decreasing curve, with a sample frequency f related to the distance between each channel (d), the sample radius (R), and the rotating speed (ω).

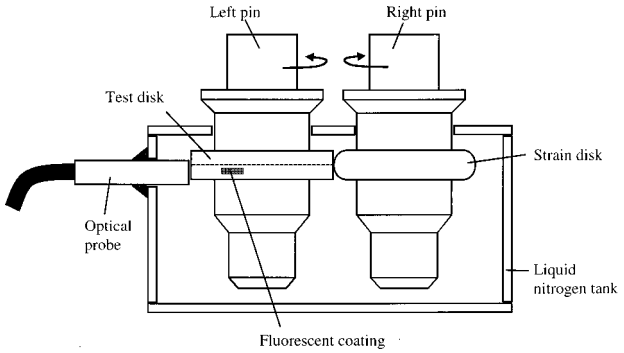

FIG. 3. Setup of the cryotribometer. The left pin is fitted with the test disk and the right pin is fitted by the strain disk. The test disk receives the fluorescent coating, and the liquid-nitrogen tank receives the optical probe.

We studied the influence of the noise level in the decay time (and so, the temperature) maximum error evaluation. As shown in Fig. 4, the minimum decay time is produced when the noise is maximum on the first pulse and minimum in the second pulse, and vice versa. The difference between the two values (the maximum scattering) depends on the noise level, the real value of the decay time, the distance between each channel, and the rotation speed. We set the signal-to-noise ratio to 20 dB, the rotating speed to 3000 rpm, and the fluorescence decay time to 340 μs (that corresponds to a temperature of 77 K), and we calculated the maximum measurement scattering versus the distance between each channel. The corresponding curve is given in Fig. 5. The maximum measurement scattering was minimum for a distance of 2.7 mm between each channel. Then, the distance between each channel is set to 2.7 mm, and the maximum measurement scattering versus temperature and rotation speed is calcu-

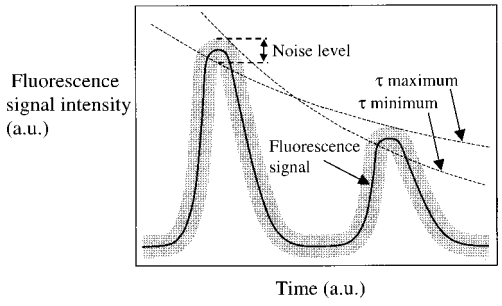

FIG. 4. Influence of the noise level in the decay time evaluation for a three-channel probe. The minimum decay time is obtained when the noise is maximum on the first pulse and minimum in the second pulse, and vice versa. The difference between the two values is the measurement scattering.

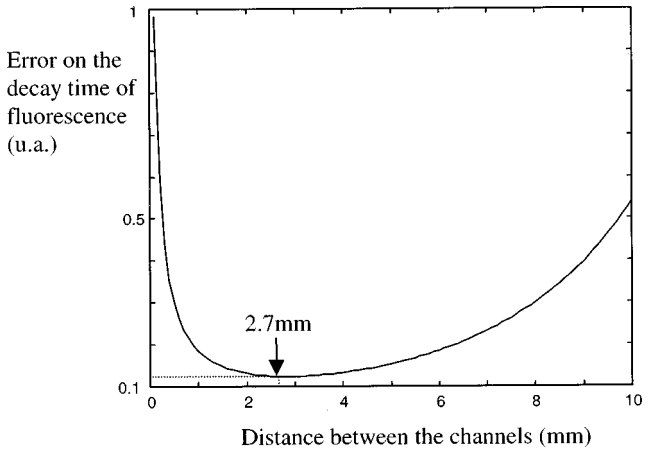

FIG. 5. Influence of the distance between each channel (d) on the measurement scattering for a three-channel probe. The calculation is made with a sample diameter of 30 mm, a rotating speed of 3000 rpm, a decay time of 340 μs, and a signal-to-noise ratio of 20 dB. For those parameters (which correspond to the middle of the expected range), the optimum distance between each fiber is 2.7 mm.

lated. The same process has been made with a probe incorporating a higher number of channels, showing that the maximum measurement scattering is proportional to the invert of the number of detection channels. Elsewhere, the optimum distance between each fiber of a five-channel probe is smaller than the fiber's diameter. This implies the use of a three- or a four-channel probe. Though the choice of a four-channel probe instead of a three-channel probe would lead to a 33% precision improvement, we have chosen a three-channel probe as it was easier to construct.

One can notice that as the intensity of the fluorescence source is decreasing, the maxima of the signal pulses do not occur when the source is just in front of the detection channels, but a few instants before. The fluorescent signal is the product of the fluorescence exponential decreasing law by the fiber response. The fiber response is the detected signal if the intensity of the fluorescent source constantly equals 1. By considering that the maxima belong to the fluorescence exponential decreasing curve, we make a systematic error, as shown in Fig. 6. The point $P(t,I)$ is the maximum of the fluorescence signal whereas the point belonging to the exponential decreasing curve is $P'(t',I')$. Nevertheless, simulations show that the relative error induced during the decay

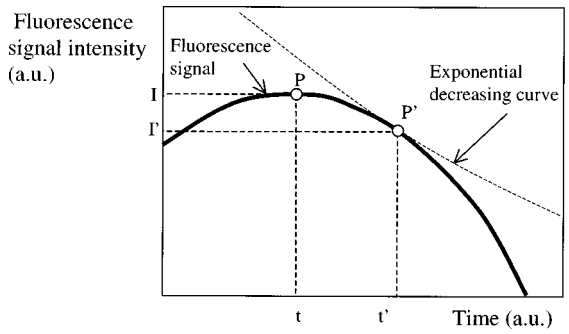

FIG. 6. Deformation of the pulse response of the detection channels. The point P' belongs to the exponential decreasing curve (dotted line). By taking into account the maximum P of the fluorescence signal (full line) in the calculation, a systematic error occurs.

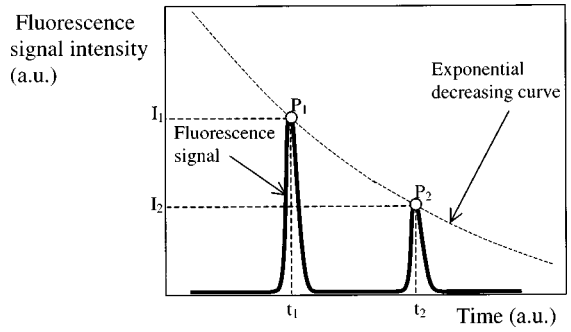

FIG. 7. Shape of the fluorescent signal with a three-channel probe. The fluorescent decay time is calculated from the coordinates t_1,t_2 and I_1,I_2 of the maxima P_1 and P_2.

time measurement is negligible dealing with the mentioned rotating speed and temperature range. Furthermore, the time delay between P and P' is smaller than the sample period (2 μs) from the middle of the rotating speed range (2500 rpm). This lead us to compute the decay time of fluorescence by considering that each pulse maximum belongs to the fluorescence exponential decreasing curve. Figure 7 shows the shape of the fluorescent signal, obtained with a three-channel probe. The coordinates t_1, t_2 and I_1,I_2 of the maxima P_1 and P_2 allow us to deduce the decay time of fluorescence τ, according to Eq. (2):

$$\tau = \frac{t_1 - t_2}{\log \frac{I_1}{I_2}}. \tag{2}$$

The coordinates t_1,t_2 are determined from the value of the rotation speed, given by the induction device of the cryotribometer, and I_1,I_2 are determined from the raw signal.

III. SETUP

We have modified a cryotribometer to implant a fluorescence temperature probe. A three-channel probe have been constructed with multimode OH^- ion-doped fibers ($\varnothing$ core $=550\,\mu$m). The width between the fibers is 2.7 mm. The diameter of the probe is 9.5 mm, with a length of 140 mm. The probe is implanted in a the liquid-nitrogen tank. The distance between the head plane of the probe and the rotating sample is adjusted to 0.3 mm. We use a specific sol–gel process [OrMoSil (Ref. 8)], to coat a rotating sample with an heterogeneous structure of sol–gel mixed with a crystalline powder of $CaF_2:Yb^{2+}$. This process give a strongly adherent gel, smooth enough to be bent without cracking during thermal shocks. It has been already demonstrated to be suitable for temperature sensing in extremes conditions.[9,10] The layer is deposited in a groove machined along the circumference (1 mm width, 0.3 mm deep), by the sol–gel process. The length of the layer was limited to 10 mm, which represents 5% of the circumference. This implies the UV excitation pulse is triggered. A nonfluorescent layer is deposited in the opposite side to counterbalance the rotation moment of the fluorescent layer. The layer is deposited above the contact

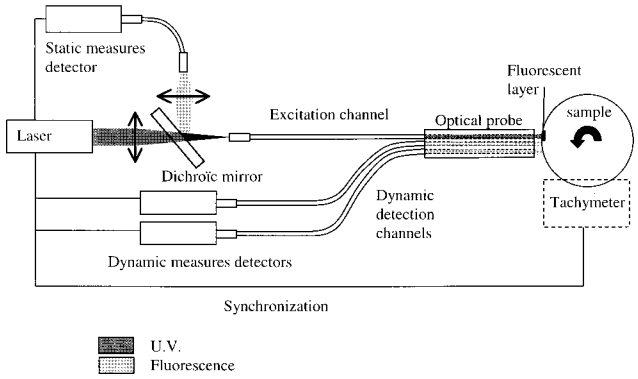

FIG. 8. Optical setup of the fluorescent temperature probe for rotating objects. The excitation UV pulse is carried out in the layer by the excitation channel. The fluorescent signal is collected by the detection channels if the sample is rotating, or by the excitation channel in the other case.

line between the two disks to prevent the layer from the friction against the strain disk, even though, we did not use the strain disk in our experience.

The complete optical setup is drawn in Fig. 8. The excitation signal is obtained with a solid-state YLF diode pumped laser, emitting pulses at 349 nm (70 μJ, 9 ns width). A dichroïc mirror allows us to split the fluorescence from the excitation pulse in the case where the excitation is used as a detection channel (if the rotating speed is null). In that case, the fluorescence signal is injected on the static detection channel. If the sample is rotating, the fluorescent signal is collected by the detection channels. Each detection channel is connected to an avalanche photodiode. The signals are sampled to 500 kHz on both of the detection channels which are connected to a PC. An electronic monitor allows us to trigger the laser source and the acquisition sequence of the computer while the layer is in front of the exciting channel. In the development phase, this detection device was used rather than an analogical device in order to compare different signal processing schemes. A later version will integrate an analogical signal processing scheme.

IV. RESULTS AND DISCUSSION

A. Calibration

A calibration probe has been built by coating the tip of an optical fiber with the heterogen fluorescent media intended to be calibrated. We use the laser source and the photodetectors described above. The single fiber both excites and collects the fluorescence signal. The fluorescence signal is separated from the excitation signal by a dichroïc mirror, and sent on a photodetector. The electric signal is sampled at 1 MHz, and the decay time is determined by a least-squares method. A helium flow cryostat gives the reference level temperature. The setup is described in Fig. 9. The mean temperature of the cryostat was determined by platinum resistors. The calibration probe described above is fixed in a shell with a reference probe. The time–temperature dispersion on the shell is limited to 10^{-4} K, but the spatial dispersion of the temperature on the shell is about 0.1 K. This limits the precision on the temperature of the probe to 0.1 K. The mean

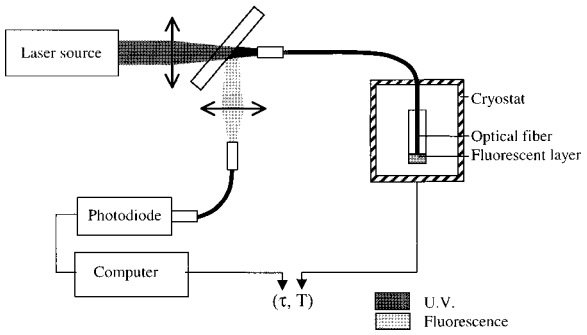

FIG. 9. Optical setup of the calibration experiments. The helium flow cryostat gives accurate temperature levels, and the decay time is calculated by a least-squares method in the sampled fluorescent signal. The mean decay time is calculated from a set of 50 measures.

decay time and the standard deviation were calculated from a 50 acquisition sequence for each calibration point. The $CaF_2:Yb^{2+}$ dye was calibrated from 60 to 130 K in steps of 10 K. Figure 10 gives a plot of the results. The circles are the experimental calibration points, the full line shows a polynomial approximation function of the calibration function.

B. Temperatures measures

We first performed measures without rotating the cylinder at 77 K. The fluorescent layer is just put in front of the exciting channel, and we used the static detection channel. The fluorescence decay time is measured and compared to the calibration curve value. The calibrated layer is not the sample's layer, but the crystal powder used for each layer is taken from the same monocrystal, and we used the same deposition process. One can assume that the calibration curve for each layer is the same, and this can be verified at 77 K in liquid nitrogen. Then, we carried out temperature measurement in liquid nitrogen under different rotation speeds. The calibration curve provides a decay time value of 338.7 μs at 77 K. At the thermal equilibrium in liquid nitrogen, the static measure of the decay time gives a value of $340 \pm 0.5\,\mu$s. The dynamic measures result in values of $344 \pm 19\,\mu$s at 2000 rpm, $326 \pm 15\,\mu$s at 3000 rpm, and $329 \pm 40\,\mu$s at 4000 rpm. The static and dynamic measures of

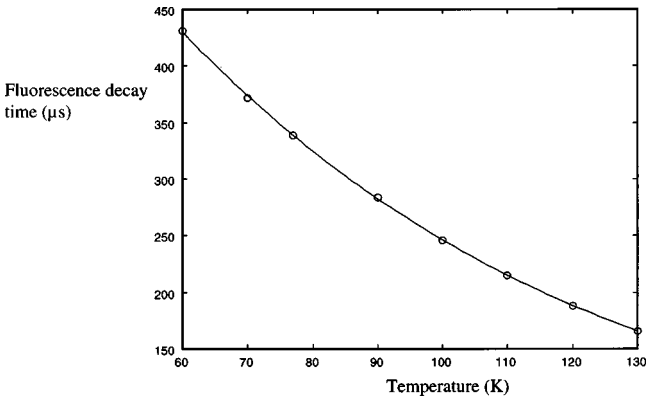

FIG. 10. Calibration curve of the fluorescent layer. The circles are the experimental points and the full line is a fifth degree polynomial approximation of the calibration function.

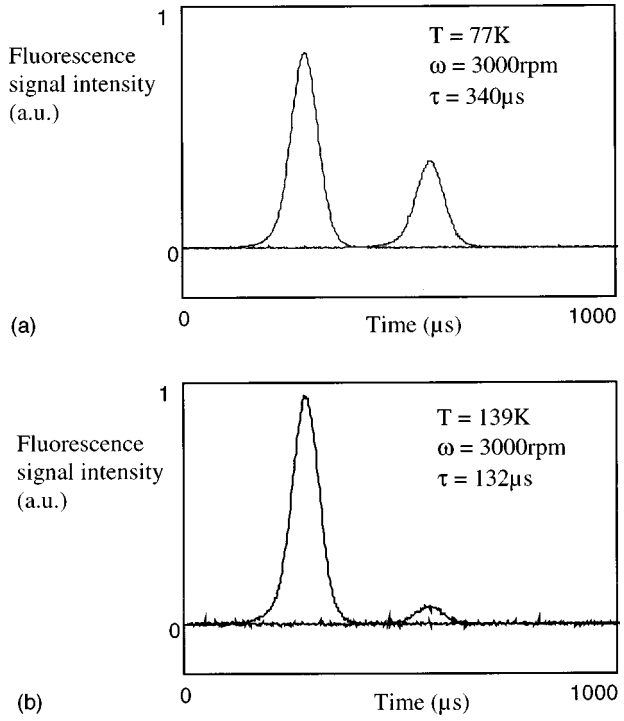

FIG. 11. Samples of fluorescent signals in dynamics measures, for a rotating speed of 3000 rpm. (a) corresponds to a temperature of 77 K; the mean decay time of fluorescence is 340 μs. (b) corresponds to a temperature of 139 K; the mean decay time of fluorescence is 132 μs. The temperatures are given by the thermocouple device.

the decay time are close to the calibration curve value. This shows that the detection channels present the same transmission coefficient furthermore, the value of the decay time dispersion leads us to expect a temperature dispersion between 3 and 10 K. Then, we used the Joule effect warm source to increase the temperature of the sample, and we compared the temperature measures given by the fluorescence method and thermocouple-based method. Figure 11 shows the fluorescent signals at 77 K [Fig. 11(a)] and 139 K [Fig. 11(b)], for a rotating speed of 3000 rpm. The corresponding decay times are, respectively, 326 and 120 μs. Figure 12 shows some significant experimental results at various temperatures and rotating speeds. The mean temperature and the standard deviation is given, according to the calibration curve. If we express the true precision as the sum of the standard deviation of the measurement expressed in temperature (Fig. 12) and the precision of the fluorescence curve (0.1 K), it appears the second term can be neglected, as it is almost an order of magnitude lower than the first. The standard deviation of the measure varies from 2 to 10 K. The values at the liquid-nitrogen temperature (77 K) are recalled. In some cases, the difference between the fluorescence temperature and the thermocouple temperature is greater than the standard deviation. This difference seems to be due to the presence of the groove and the fluorescent layer on the sample surface, that breaks the cylindrical symmetry of the sample. The thermocouple-based method assumes that the temperature is only radius dependent; and the sample temperature surface is homogeneous. Nevertheless, the groove and the layers are an inhomogeneous surface, with nucleation sites where bubbles

Rotating speed (rpm)	Thermocouples temperature (K)	Fluorescence decay time (μs)	Standard deviation on τ (μs)	Fluorescence temperature (K)	Standard deviation on the temperature (K)
0	77	340	0.5	76.7	0.1
2000	77	344	19	75.8	3.7
3000	77	326	15	78.8	3.3
4000	77	329	40	79.2	8.6
2000	80	348	12	74.9	2.6
3000	82	326	17	79.7	3.7
2000	117	320	9	81.1	2.0
4000	145	258	34	96.8	10.0
4000	145	164	20	130.5	9.1

FIG. 12. Experimental results. The precision on the mean temperature surface given by the thermocouple method is 0.5 K, since the surface temperature is homogeneous. The mean temperature and the measurement scattering of the fluorescence method are given for each measure.

are preferentially forming. This leads to a surface temperature gradient, taken into account by the fluorescence method (close to a punctual measurement), and not by the thermocouple method (average measurement).

C. Discussion

Compared to the thermocouple ones, our method has the advantage of being a direct method. Yet, the presence of the layer disturbs the measure, as the uncoated sample is a system whose thermodynamic behavior is different from the coated sample (machined groove, fluorescent, and nonfluorescent layers). Nevertheless, it is for some cases (ball bearings, turbopump axis) the only alternative to simulation. The precision is quite bad compared to the thermocouple precision, but it can be much better than simulations. There are two main problems related to the influence of the layer. On one hand, the layer modifies the warm exchange coefficient between the liquid nitrogen and the sample. This modifies the surface temperature of the sample. The second problem is that we measure the temperature of the layer and not that of the sample surface. While those temperatures are the same at the thermal equilibrium, a difference exists if there are warm exchanges even in a permanent or a transitory rate. A convenient way to reduce this influence is to reduce the dimensions of the layer (surface and thickness), and to choose a fluorescence media whose thermodynamic characteristics are close to the sample's. Elsewhere, a complete study of this problem has led to the knowledge of the thermal characteristics of the layer. This is difficult because of its heterogeneous nature.

The application of fluorescence thermometry both to the cryogenic range and rotating samples extend the field of the method. A more reliable way to increase the intrinsic precision of the method is to increase the number of detection channels. This can be achieved by using a four-channel fiber or a greater number of fibers with a smaller core diameter. As said above, a four-channel fiber could reduce the measurement dispersion by about 25%, but a higher number of smaller fibers will not necessarily increase the precision as the signal-to-noise ratio will be reduced. However, the goal of our method is the monitoring of turbopump axis temperature, whose rotating speed range is an order of magnitude greater than the cryotribometer's. In this case, the probe can include ten times more fiber with the same signal-to-noise ratio. The use of an analogical detection device will resolve the problem of the resolution of the pulses. The reached per-

formance at a few thousand rpm (from 2 to 10 K) lets us assume than we could reach a temperature dispersion of about 0.2 K by using ten times more points of measure and a least-squares method, at a few ten thousand rpm.

ACKNOWLEDGMENTS

The authors gratefully thank Professor H. Bill of the University of Geneva; Professor G. Boulon of the University of Lyon for helpful discussions and supplying the fluorescent crystals; Professor P. Audebert of ENS (Paris) for the sol–gel process contribution; Dr. P. Chantrenne of INSA (Lyon), where the thermocouple method temperature measurements were performed; and G. Tribillon and J. Rolland for their helpful contribution.

[1] K. T. V. Grattan and Z. Y. Zhang, *Fiber Optic Fluorescence Thermometry* (Chapman and Hall, London, 1995).
[2] Z. Zhang, K. T. V. Grattan, and A. W. Palmer, Proc. SPIE **1885**, 300 (1993).
[3] A. T. Augousti, K. T. V. Grattan, and A. W. Palmer, J. Lightwave Technol. **5**, 759 (1987).
[4] Z. Zhang, K. T. V. Grattan, and A. W. Palmer, Rev. Sci. Instrum. **63**, 3177 (1992).
[5] B. Moine, B. Courtois, and C. Pedrini, J. Lumin. **48**, 501–504 (1991).
[6] S. Bertrand, A. Jalocha, G. Tribillon, M. Bouazaoui, and J. Rouhet, Opt. Laser Technol. **28**, 363 (1996).
[7] J. Rouhet, G. Tribillon, S. Bertrand, and G. Boulon, Dispositif de mesure optique de température cryogénique, Patent No. 9409797, France (1994).
[8] C. J. Brinker, and G. W. Scherer, *Sol–Gel Science. The Physics and Chemistry of Sol–Gel Processing* (Academic, New York, 1990).
[9] S. Bertrand, F. Bresson, P. Audebert, and G. Tribillon, Opt. Commun. **117**, 90 (1995).
[10] P. Audebert, S. Bertrand, F. Bresson, and G. Tribillon, Appl. Surf. Sci. **119**, 207 (1997).